

Thomas precession, persistent spin currents and quantum forces

S.Ouvry,¹ L.Pastur,² and A.Yanovsky²

¹*LPTMS, CNRS UMR 8626, Faculté des Sciences d'Orsay, Orsay 91405 France*

²*B. Verkin ILTPE, NAS of Ukraine, 47 Lenin Ave, Kharkov 61103 Ukraine*

We consider T-invariant spin currents induced by spin-orbit interactions which originate from the confined motion of spin carriers in nanostructures. The resulting Thomas spin precession is a fundamental and purely kinematic relativistic effect occurring when the acceleration of carriers is not parallel to their velocity. In the case, where the carriers (e.g. electrons) have magnetic moment the forces due to the electric field of the spin current can, in certain conditions, exceed the van der Waals-Casimir forces by several orders of magnitude. We also discuss a possible experimental set-up tailored to use these forces for checking the existence of a nonzero anomalous magnetic moment of the photon.

PACS numbers: 85.75.-d, 75.76.+j, 71.70.Ej, 81.07.Gf, 85.85.+j, 85.35.-p, 73.22.Gk, 73.63.-b

I. INTRODUCTION

The studies of the electronic spin degrees of freedom, spintronics, is an active branch of solid state physics. In particular, spintronics of nanostructures, or nanospintronics, has developed quite rapidly in recent years,¹⁻³ motivated by a number of basic questions on the nature of nanophenomena as well as by its potential impact on information technology. The underlying physical mechanism is the spin-orbit interaction of conducting electrons, which couples their spin degree of freedom to their orbital dynamics.

One distinguishes the extrinsic phenomena, the result of spin dependent scatterings on (external) impurities, from the intrinsic phenomena, arising because of a certain spin-orbit coupled band structure. There are two basic dynamical mechanisms underlying intrinsic phenomena in semiconductors: (i) the Rashba⁴ coupling due to the combined effects of atomic spin-orbit coupling and structured inversion asymmetry; (ii) the Dresselhaus⁵ coupling due to the bulk crystal inversion asymmetry.

The intrinsic spin-orbit interactions are essential for many potential applications like spin polarized currents without magnetism,⁶ spin field-effect transistor,⁷ topological insulator states,^{8,9} etc. One of the important spin-orbit effects in nanostructures is the persistent spin currents arising from the above dynamical sources of asymmetry, see e.g.^{10,11}

In this article we consider yet another mechanism for spin-orbit coupling whose origin is the Thomas spin precession¹²⁻¹⁶ a fundamental relativistic effect. It occurs when the particles acceleration is not parallel to their velocity, i.e. for any motion of relativistic particles with curving or winding trajectories. The precession has a purely kinematical origin since it results solely from the confined motion of the particles in a sufficiently small volume. It is not necessary related to impurity scatterings or other extrinsic¹⁷⁻¹⁹ spin-orbit mechanisms. Likewise, the Thomas precession can occur even for ideal metallic nanoparticles without Rashba or Dresselhaus couplings. As we will show below, the Thomas precession will in-

duce persistent spin currents whose dependence on the spin degree of freedoms and on the quantum spectrum is different from those resulting from the Rashba-Dresselhaus couplings.

The inverse asymmetry (the broken P -invariance) is the cause of spin persistent currents due to spin-orbital coupling. However, time reversal invariance (T -invariance) is not broken in this case. This is in complete agreement with the symmetry of pure spin (or other rotation) equilibrium currents, which are obviously not P -invariant but are T -invariant. Indeed, any geometric constraint breaks P -invariance.

A confining strip as an example of geometry in which there exist the winding persistent spin currents due to the Thomas precession has been already considered in Ref.²⁰ in the case of classical Brownian motion.

In this paper we discuss a quantum phenomenon in nanostructures, whose origin is also the Thomas precession. In this case the P -invariance with respect to winding and spin is also absent because of the confined motion of carriers.

II. THOMAS PRECESSION IN NANOSTRUCTURES

We consider an ideal and neutral metallic wire as an example of Thomas precession due to the confinement of particles. Clearly if the wire were straight, the motion of free electrons along the wire would have no relation to precession and spin-orbit interactions. If, however, the wire is curved into a closed loop, then the motion of electrons along the loop will inevitably produce the Thomas precession of their spins. Note that there is no electric field in this case and the wire is neutral and equipotential.

Let us estimate the order of magnitude of spin-orbit effects resulting from Thomas precession in a loop of nanosize assuming for simplicity that the loop is a ring. In the leading relativistic approximation the spin-orbit energy

from Thomas precession is^{12,14}

$$E_{s-o} \approx \frac{\vec{s} \cdot (\vec{v} \times \dot{\vec{v}})}{2c^2} = \frac{v^2}{2c^2} \vec{s} \cdot \dot{\vec{\theta}}. \quad (1)$$

Here the over-dot denotes the time derivative, \times the vector product, c the speed of light, \vec{s} the particle spin in angular momentum units, \vec{v} its velocity and $\vec{\theta}$ its winding angle defined as

$$\vec{\theta} = \int_0^t \frac{\vec{v} \times \dot{\vec{v}}}{v^2} dt.$$

It is the vector sum of all the windings of the particle trajectory (see²⁰). The acceleration of the winding modes in a ring at constant angular velocity is simply $\dot{v} = v^2/r$ where r is the radius of the ring. Comparing (1) with the commonly used estimate $e\vec{s} \cdot (\vec{v} \times \vec{\mathcal{E}}_{eff})/2mc^2$ of the spin-orbit energy in an electric field $\vec{\mathcal{E}}_{eff}$, where e and m are respectively the charge and the mass of the particle,²¹ we conclude that the Thomas precession of a free electron inside a metallic nanoring corresponds to a velocity dependent effective electric field

$$\mathcal{E}_{eff} \sim \frac{mv^2}{er}. \quad (2)$$

Typically for electrons in metals the Fermi energy ε_F is of the order of several electronvolts (e.g. $\varepsilon_F \sim 6$ eV for Au), hence the Fermi velocity is $v_F \sim 10^6$ m/s. Thus, in the case of nanoring, where $r \sim 10^{-9} \div 10^{-8}$ m and the particle velocity is of the order of the Fermi velocity $v \sim v_F$, the effective electric field in (2) can be quite large, i.e., $\mathcal{E}_{eff} \sim 10^{10}$ V/m. We conclude that the spin-orbit effects can be well pronounced in nanorings. Note again that the electric field is just an "effective" field arising from the trajectory windings and there is no gradient of an electrical potential along a metallic nanoring.

Let us now show that the spin-orbit coupling (1) due to Thomas precession leads to persistent spin currents. Note that we are using here a 1d ring and non interacting fermions to obtain simple estimates, keeping in mind that we are interested in 2d or 3d nanostructures.

The effective classical Lagrangian of free electrons which takes into account the Thomas precession is^{13,16}

$$L = -mc^2 \sqrt{1 - \frac{v^2}{c^2}} - \vec{s} \cdot \left(\frac{1}{\sqrt{1 - \frac{v^2}{c^2}}} - 1 \right) \frac{\vec{v} \times \dot{\vec{v}}}{v^2} \quad (3)$$

Note that the low velocity expansion of the second term in the r.h.s of (3) rightly reproduces (1). In the simple ring geometry we have in general

$$\vec{v} = r\dot{\theta}\vec{e}_\theta \quad (4a)$$

$$\dot{\vec{v}} = -r^{-1}v^2\vec{e}_r + r\dot{\theta}\vec{e}_\theta, \quad (4b)$$

where θ is the polar angle, \vec{e}_θ and \vec{e}_r are the polar unit vectors in the plane of the ring. It follows that for the

ring geometry

$$\frac{\vec{v} \times \dot{\vec{v}}}{v^2} = \dot{\theta}\vec{e}_z \quad (5)$$

where \vec{e}_z is the unit vector of the z -axis perpendicular to the ring, so that the winding angle and the polar angle are equal, thus denoted by the same symbol θ). We obtain from (3)

$$L = -mc^2 \sqrt{1 - \frac{r^2\dot{\theta}^2}{c^2}} - \left(\frac{1}{\sqrt{1 - \frac{r^2\dot{\theta}^2}{c^2}}} - 1 \right) s_z \dot{\theta} \quad (6)$$

where s_z is the spin projection on \vec{e}_z . Note that the double derivative $\ddot{\theta}$ in (4b) does not contribute to the r.h.s. of (6). Nevertheless the quantization of (6) is quite non-trivial. Fortunately, in the case of non interacting fermions, we can neglect states above the Fermi energy assuming for simplicity zero temperature, i.e. $r\dot{\theta} = v \leq v_F \ll c$. Thus, expanding the r.h.s. of (6) in the small parameter $v_F/c \sim 10^{-2}$ and dropping the constant energy $-mc^2$, we obtain

$$L \approx \frac{mr^2\dot{\theta}^2}{2} - s_z \frac{r^2\dot{\theta}^3}{2c^2}, \quad r\dot{\theta} \ll c. \quad (7)$$

The angular momentum p_θ plays for (6) the role of a generalized momentum

$$p_\theta = \frac{\partial L}{\partial \dot{\theta}} \approx mr^2\dot{\theta} - \frac{3}{2}s_z \frac{r^2\dot{\theta}^2}{c^2}. \quad (8)$$

Taking into account that $p_\theta \ll mrc \ll m^2r^2c^2/\hbar$ (the second inequality means that the quantum uncertainty of the velocity \hbar/mr has to be much smaller than c), i.e., $\dot{\theta} \ll c/r \ll mc^2/\hbar$, we can express $\dot{\theta}$ as

$$\dot{\theta} \approx \frac{p_\theta}{mr^2} + \frac{3}{2} \frac{s_z}{m^3r^4c^2} p_\theta^2 \quad (9)$$

Thus, using (7) and (9), the Hamiltonian corresponding to (6) is

$$H = p_\theta \dot{\theta} - L \approx \frac{p_\theta^2}{2mr^2} + \frac{1}{2} \frac{s_z p_\theta^3}{m^3r^4c^2} \quad (10)$$

Now the standard quantization procedure

$$p_\theta \rightarrow \hat{p}_\theta = -i\hbar \frac{\partial}{\partial \theta}, \quad s_z \rightarrow \hat{s}_z = \frac{\hbar}{2} \hat{\sigma}_z. \quad (11)$$

yields the quantum Hamiltonian

$$\hat{H} = -\frac{\hbar^2}{2mr^2} \frac{\partial^2}{\partial \theta^2} + i\frac{1}{4} \frac{\hbar^4}{m^3r^4c^2} \hat{\sigma}_z \frac{\partial^3}{\partial \theta^3}. \quad (12)$$

Its spectrum has doubly degenerated energy levels

$$\epsilon_{n\sigma_z} = \frac{\hbar^2 n^2}{2mr^2} + \frac{\hbar^4 \sigma_z n^3}{4m^3r^4c^2}, \quad (13)$$

$$\sigma_z = \pm 1, \quad n = 0, \pm 1, \pm 2, \dots,$$

since $\epsilon_{n,\sigma_z} = \epsilon_{-n,-\sigma_z}$, and two-component states

$$\Psi_{n,\sigma_z} = \frac{1}{4\pi} e^{in\theta} \begin{pmatrix} 1 + \sigma_z \\ 1 - \sigma_z \end{pmatrix}. \quad (14)$$

Eqs. (13)-(14) can be used only for the winding numbers n satisfying (cf. (7) and (9))

$$|n| < N \ll \frac{mcr}{\hbar}, \quad (15)$$

where

$$N \approx \frac{r\sqrt{2m\varepsilon_F}}{\hbar} \quad (16)$$

is a natural cutoff fixed by the Fermi energy, i.e. $\epsilon_{N\sigma_z} \leq \varepsilon_F < \epsilon_{N+1\sigma_z}$. With $r \sim 1$ nm we have roughly $N \sim 10 \div 100$. Hence, N is large but still much smaller than $mcr/\hbar \sim 10^3$, and (15) holds. In addition, the spacing between levels ~ 0.1 eV i.e. ~ 1000 Kelvin is such that the zero temperature approximation is still valid at room temperature.

To find the operator of the spin current we use again the standard procedure based on the time derivative of the spin density observable \vec{s} , see e.g.²³⁻²⁵ (other approaches are also possible, see e.g.²⁸)

$$\frac{d}{dt} \vec{s} \equiv \frac{d}{dt} \Psi^\dagger \hat{s} \Psi = \frac{1}{i\hbar} \left[\Psi^\dagger \hat{s} \hat{H} \Psi - (\hat{H} \Psi)^\dagger \hat{s} \Psi \right], \quad (17)$$

where Ψ is the wave function. Using (10)–(12), we obtain in the coordinate representation (recall that in our case the coordinate is the winding angle θ) the continuity equation

$$\frac{d}{dt} s_i = -\frac{1}{r} \frac{\partial}{\partial \theta} \Psi^\dagger \hat{J}_{\theta,i} \Psi \quad (18)$$

where $\hat{J}_{\theta,i}$ is the i th component of the spin 1d current operator circulating in the ring

$$\hat{J}_{\theta,i} = \frac{1}{2} \left\{ \frac{\hat{p}_\theta}{mr} - \frac{\hat{s}_z \hat{p}_\theta^2}{m^3 r^3 c^2}, \hat{s}_i \right\} = \frac{\{\hat{v}_\theta, \hat{s}_i\}}{2}. \quad (19)$$

Here $\{\cdot, \cdot\}$ is the anticommutator and \hat{v}_θ can be viewed as the spin velocity.

Using the spectrum (13) and the eigenstates (14), we find that in the leading N^{-1} approximation the only non-vanishing component of the spin current density is that in the z direction

$$\begin{aligned} \vec{j} &= \frac{1}{r} \sum_{n=-N}^N \sum_{\sigma_z=\pm 1} \Psi_{n,\sigma_z}^\dagger \hat{J}_{\theta,z} \Psi_{n,\sigma_z} \approx \\ &\sum_{n=-N}^N \sum_{\sigma_z=\pm 1} \Psi_{n,\sigma_z}^\dagger \frac{\hbar^2 \hat{\sigma}_z^2 \hat{p}_\theta^2}{4m^3 r^4 c^2} \Psi_{n,\sigma_z} \approx \\ &\frac{1}{3} \frac{\hbar^4}{m^3 r^4 c^2} \left(\frac{r\sqrt{2m\varepsilon_F}}{\hbar} \right)^3 \quad (20) \end{aligned}$$

The current is protected by the T -invariance. Indeed, the current dissipation requires the backscatterings without spin-flip, which are impossible since the higher winding numbers are too distant (remember that the energy level spacings are $\sim 100 \div 1000$ K). Besides, all the states below the Fermi energy are occupied. As a result, the backscatterings with spin-flip contribute only to the same spin current.

An important fact is that the whole spectrum (13) – (16) contributes to (20) (except the levels with zero winding number). Note that one can rewrite (20) as

$$\vec{j} \sim \frac{8\pi}{3} \frac{\hbar}{mr} N \frac{\varepsilon_F}{mc^2} \frac{\hbar}{2} \frac{1}{2\pi r} \sim \hbar \left(\frac{v_F}{c} \right)^2 \frac{v_F}{r} \quad (21)$$

One obtains an estimate for \vec{j} as a constant times the velocity quantum uncertainty $\delta v \sim \hbar/mr$, the Fermi level number N , the relativistic factor $\varepsilon_F/(mc^2)$, the spin momentum $\hbar/2$, divided by the length of the ring $2\pi r$. Thus, the spin current results from the combination of geometric, quantum and relativistic effects.

It follows also from (21) that the current density is decays in r , so that it could become negligible at a macroscopic scale. If, however, we consider a "metamaterial", i.e., a macroscopic sample paved by a big number of nanorings, then the resulting spin current can be quite large (a sample area of the order of 1 mm^2 can contain up to 10^{12} of such nanorings).

It is known that the current of magnetic moment can produce an electric field decaying as R^{-3} in the distance R from the current or as R^{-2} in the case of spin rotation^{22,25}. This field $\vec{\mathcal{E}}$ can be estimated by using Lorentz force in the rest frame of the spin, i.e. via the transformation rules for a magnetic field in the rotating reference frame

$$\vec{\mathcal{E}} \approx -(\dot{\theta} \times \vec{R}) \times \vec{B}. \quad (22)$$

Here \vec{B} is the magnetic field induced by the electron magnetic moment in the rest frame and it is assumed that $R \gg r$ and $\dot{\theta} \ll c/R$, i.e., that the distance from the ring is much larger than its size and the rotation is slow enough. In fact the validity of the formula is a rather delicate issue (see e.g. the review²⁶ and references therein), but we believe that the formula provides a correct order of magnitude in our estimates. Since the magnetic moment of an electron with spin s_z is $g\mu_B s_z/\hbar$, where $g \sim 2$ is the gyromagnetic factor and $\mu_B = e\hbar/(2m)$ is the Bohr magneton, the magnetic field induced by s_z in the rest frame is (cf.²²)

$$\vec{B} \approx -\frac{g\mu_0\mu_B s_z}{2\pi\hbar} \frac{\partial}{\partial \vec{R}} \frac{Z}{R^3}, \quad Z = \vec{e}_z \cdot \vec{R} \quad (23)$$

Replacing here $\dot{\theta} s_z$ by $2\pi\vec{j}$ and using (20)-(23), we obtain the electric field in the laboratory reference frame

$$\vec{\mathcal{E}} \sim \frac{\mu_0 g \mu_B}{3rc^2} \left(\frac{2\varepsilon_F}{m} \right)^{\frac{3}{2}} \left(\frac{\vec{R} + 2Z\vec{e}_z}{R^3} - 3\frac{Z^2\vec{R}}{R^5} \right) \quad (24)$$

This leads to

$$\mathcal{E} \sim \frac{4\mu_0\mu_B}{3rR^2} \frac{\varepsilon_F}{mc^2} v_F \quad (25)$$

so that $\mathcal{E} \sim 10^{-2} \div 1 \text{ V m}^{-1}$ at the nanoscale ($R \sim 1 \div 10 \text{ nm}$), i.e. it is comparable or bigger than the electric field $\sim 10^{-2} \text{ V m}^{-1}$ obtained¹⁰ at a distance 5 nm from a Rashba ring. It is also worth noting that the electric field due to Thomas precession may exist in any (not necessarily metallic) nanoparticle which confines magnetic moments in motion. Note also that (18)-(25) have been derived for a constant curvature: we believe, however, that the same conclusions can essentially be reached in the case of a non constant curvature.

Let us finally compare the electric force $F_T = e\mathcal{E}$ acting on the charge carrier due to Thomas spin precession and the electric force F_C due to the van der Waals-Casimir effect, the only known so far electric force in metallic devices under the conditions of equilibrium and neutrality. According to²⁹

$$F_C \sim \frac{7c_0}{\pi} \frac{\hbar cr^6}{R^8}, c_0 = \frac{143}{16} \quad R \gg r \quad (26)$$

It follows then from (25) and (26)

$$\frac{F_T}{F_C} \sim \frac{4\pi}{21c_0} \frac{e\mu_0\mu_B v_F R^6}{\hbar cr^7} \frac{\varepsilon_F}{mc^2} \quad (27)$$

Let R_0 be the distance where the Thomas force and the van der Waals-Casimir force are equal: from (27) one has

$$R_0 \sim \left(\frac{mc^2}{\varepsilon_F} \frac{\hbar cr}{e\mu_0\mu_B v_F} \right)^{\frac{1}{6}} r, \quad (28)$$

so that taking $r \sim 1 \text{ nm}$ one gets $R_0 \sim 10^2 \text{ nm}$. In other words, Thomas precession forces may dominate van der Waals-Casimir forces for distances from 10^2 nm and larger. It has already been mentioned above that using "metamaterials" (pavements of macroscopic devices by nanoparticles) one can obtain forces proportional to the area of the macroscopic sample.

III. ON A POSSIBLE EXPERIMENT ON THE ANOMALOUS MAGNETIC MOMENT OF THE PHOTON

We have so far considered electrons because they possess a non-zero magnetic moment. On the other hand, photons have zero magnetic moment despite their spin being 1. Nevertheless, there are theoretical arguments (see e.g.^{31,32} and references therein) according to which the photon has an anomalous magnetic moment μ_γ . It is clear, however, that any experimental proof of this fact has to be fairly sophisticated. For instance, the use of inhomogeneous magnetic fields for direct measurements would require extremely strong fields in view of a very large c and a very small μ_γ .

We would like to point out that the appearance of an electric field from the photon magnetic moment due to Thomas precession could provide a way to check whether $\mu_\gamma \neq 0$.

One has to consider normal (non-persistent) photon currents. To this end one could use light guides with polarized light or recently found 100% reflective materials³⁰ and measure the electric field from the confinement of light in small volumes. In this case, however, it would be quite difficult to detect the contribution of the μ_γ current from other possible sources of the electric field. The idea is to use an initially unpolarized source of light and two light guides: one with a "constructive" winding of light and the other with a "destructive" (compensating) winding, as shown in Figure 1.

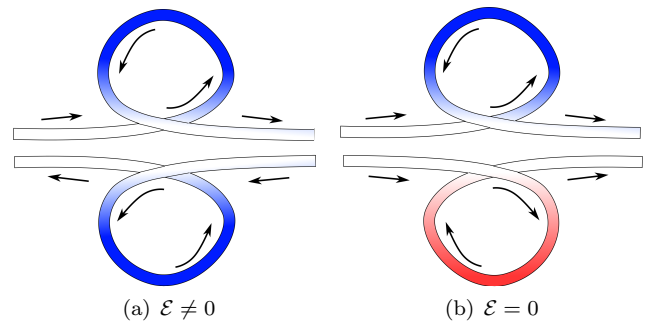


FIG. 1. (a) – light guide with nonzero spin current due to "additive" winding. (b) – light guide with "destructive" winding. The blue and red colors denote opposite spin precessions.

In this case one does not need to separate the contribution of the μ_γ -current to the electric field from those stemming from other sources, since the unique difference in the two light guides is their winding directions, hence their Thomas currents, and so one has simply to compare their electric fields. To estimate the effect we assume that the refraction coefficient $n = c/v$ of the light guide medium is $1.5 \div 2$ (optical glasses, crystals, etc), where v is the speed of light in the medium. We consider UV light with a wavelength $\lambda \sim 100 \text{ nm}$ and micro-meter windings with $r \sim 1 \mu\text{m}$. In this case the spin-orbit energy of the Thomas precession is still less than the kinetic energy and we can use the formula

$$E_{s-o} \sim \frac{v^2}{2c^2} s\dot{\theta} \sim \frac{\hbar c}{2n^3 r} \ll \frac{\hbar c}{\lambda}$$

which doesn't contain μ_γ . Hence, the effective magnetic field

$$B \sim \frac{E_{s-o}}{\mu_\gamma} \sim \frac{\hbar c}{2n^3 r \mu_B} \frac{\mu_B}{\mu_\gamma} \sim \frac{10^5}{2} \frac{\mu_B}{\mu_\gamma} \text{ Tesla} .$$

acting on μ_γ is quite strong.

It follows that Thomas precession could be used in order to detect μ_γ even if it is very small. Indeed, the resulting photonic spin current j_γ can be estimated as

$$j_\gamma \sim \rho_\gamma \hbar \frac{E_{so}}{p} \sim \rho_\gamma \hbar \frac{\lambda c}{n^3 r}$$

where $p = h/\lambda$ is the photon momentum and ρ_γ is the 1d photon density. The electric field due to Thomas precession follows by repeating the same steps as in (24) with $g\mu_B$ replaced by μ_γ and \vec{j} by j_γ

$$\mathcal{E}_\gamma \sim \frac{\mu_0 \mu_\gamma j_\gamma}{\hbar R^2} \sim \mu_0 \rho_\gamma \mu_\gamma \frac{\lambda c}{n^3 r R^2}.$$

Therefore, μ_γ can be detected from the measurements of \mathcal{E}_γ for a sufficiently dense array of curved light circuits.

We can compare the electric field \mathcal{E}_γ obtained here and the electric field \mathcal{E} derived above for electrons in a metal nanoring of the same radius

$$\frac{\mathcal{E}_\gamma}{\mathcal{E}} \sim \rho_\gamma \lambda \frac{\mu_\gamma}{\mu_B} \left(\frac{c}{v_F} \right)^3 \frac{1}{n^3}$$

We see that a very small value of μ_γ/μ_B can be in part compensated by the cube of the inverse relativistic factor v_F/c .

We have presented above estimates for winding effects in light guide experiments. Similar effects could as well show up in the winding of diffuse light and the associated magnetic moment edge currents for the strip geometry considered in.²⁰

IV. CONCLUSION

We have shown that the Thomas precession resulting from the confined motion of spins carriers can generate some specific persistent spin currents. For the sake of concreteness, we have considered conducting electrons in metallic nanorings. It was pointed out, however, that similar effects can be expected for other spin carriers like magnons, spinons, ions in gases, etc. The Thomas precession of magnetic moments can generate electric forces that are stronger than the usual van der Waals-Casimir forces in metallic samples. Hence, it seems certainly appropriate to take Thomas precession effects into account when dealing with metallic nanoparticles. It has also been suggested that the electric forces due to Thomas precession can be a possible tool for experimentally testing the existence (see^{31,32} and references therein) of a non-zero anomalous magnetic moment for the photon.

V. ACKNOWLEDGMENT

This work was partly supported by the French-Russian program "Dnipro 2013-2014" (CNRS – NASU). A. Yanovsky would like to thank the Laboratory of Theoretical Physics and Statistical Models (LPTMS) of CNRS, University Paris Sud for hospitality during the initial stage of the work.

-
- ¹ A. Bernand-Mantel, P. Seneor, N. Lidgi, M. Muñoz, V. Cros, S. Fusil, K. Bouzehouane, C. Deranlot, A. Vaures, F. Petroff, and A. Fert, *Appl. Phys. Lett.* **89**, 062502 (2006).
² P. Seneor, A. Bernand-Mantel and F. Petroff, *Journal of Physics: Condensed Matter* **19**, 165222 (2007).
³ T. Kontos and A. Cottet, *Europhysics News* **38**, 28-30 (2007).
⁴ E. Rashba, *Fiz. Tverd. Tela (Leningrad)* **2**, 1224 (1960), [*Sov. Phys. Solid State* **2**, 1109 (1960)].
⁵ G. Dresselhaus, *Phys. Rev.* **100**, 580 (1955).
⁶ D. Awschalom, N.Samarth, *Physics* **2**, 50 (2009).
⁷ S. Datta, B. Das, *Appl. Phys. Lett.* **56**, 665 (1990).
⁸ C. L. Kane and E. J. Mele, *Phys. Rev. Lett.* **95**, 146802 (2005).
⁹ M. Z. Hasan and C. L. Kane, *Rev. Mod. Phys.* **82**, 3045 (2010).
¹⁰ Qing-feng Sun, X. C. Xie, Jian Wang, *Phys. Rev. B* **77**, 035327 (2008).
¹¹ S. K. Maiti, S. Sil, A. Chakrabarti, *Phys. Lett. A* **376**, 2147 (2012).
¹² L. H. Thomas, *Nature* **117**, 514 (1926).
¹³ Ya. I. Frenkel, *Zeitschrift für Physik* **37**, 243 (1926), detailed version in Ya. I. Frenkel, *Works*, vol 2, p. 460, Acad. Sci. of USSR, Moscow, 1958
¹⁴ J. D. Jackson, *Classical Electrodynamics*, (Wiley Inc., 1998) p. 808.
¹⁵ S.-I. Tomonaga, and T. Oka, *The Story of Spin*, (University of Chicago Press, 1997)
¹⁶ I.M.Ternov, V.A.Bordovitsyn, *Sov. Phys. Usp.* **23**, 679-683 (1980)
¹⁷ H.-A. Engel, B. I. Halperin, and E. I. Rashba, *Phys. Rev. Lett.* **95**, 166605 (2005).
¹⁸ W.-K. Tse and S. Das Sarma, *Phys. Rev. Lett.* **96**, 056601 (2006).
¹⁹ N. P. Stern, D. W. Steuerman, S. Mack, A. C. Gossard, and D. D. Awschalom, *Nature Physics* **4**, 843 (2008)
²⁰ S. Ouvry, L. Pastur, A. Yanovsky, *Phys. Lett. A* **377**, 804 (2013).
²¹ J. D. Bjorken and S. D. Drell, *Relativistic Quantum Mechanics*, McGraw-Hill, Inc., N.-Y. (1964), Section 4.3.
²² Qing-feng Sun, Hong Guo, and Jian Wang, *Phys. Rev. B* **69**, 054409-054414 (2004).
²³ U. Zülicke and C. Schroll, *Phys. Rev. Lett.* **88**, 029701 (2002).
²⁴ J. Splettstoesser, M. Governale, and U. Zülicke, *Phys. Rev. B* **68**, 165341 (2003).
²⁵ Qing-feng Sun, and X. C. Xie, *Phys. Rev. B* **72**, 245305 (2005).
²⁶ K. T. McDonald. (2008). "Electrodynamics of rotating systems" available online at the site: <http://www.physics.princeton.edu/~mcdonald/examples>
²⁷ R.Peierls, *Surprises in Theoretical Physics*, Princeton University Press, 66 p., (1979).
²⁸ R. S. Johal, *Phys. Lett. A* **263**, 62 (1999).
²⁹ T. Emig, N. Graham, R. L. Jaffe, and M. Kardar, *Phys. Rev. Lett.* **99**, 170403 (2007).

- ³⁰ Chia Wei Hsu, Bo Zhen, Jeongwon Lee, Song-Liang Chua, S. G. Johnson, J. D. Joannopoulos and M. Soljačić, *Nature* **499**, 188 (2013).
- ³¹ H. Perez Rojas and E. Rodriguez Querts, *Int. J. Mod. Phys. D* **19**, 1711, (2010).
- ³² S. Villalba-Chavez, *Phys. Rev. D* **81**, 105019 (2010)